

## Positron trapping in $Y_{1-x}Pr_xBa_2Cu_3O_{7-\delta}$ and the Fermi surface of $YBa_2Cu_3O_{7-\delta}$

A. Shukla, L. Hoffmann, A. A. Manuel, E. Walker, B. Barbiellini,\* and M. Peter

*Département de Physique de la Matière Condensée, Université de Genève, 24 Quai E. Ansermet, 1211 Genève 4, Switzerland*

(Received 12 August 1994)

Temperature-dependent positron lifetime measurements in ceramic  $Y_{1-x}Pr_xBa_2Cu_3O_{7-\delta}$  samples reveal positron trapping, in particular at low temperature and for small  $x$ . Positrons appear to be completely delocalized for  $T \sim 400$  K and higher. At high temperatures the lifetime for  $YBa_2Cu_3O_{7-\delta}$  and  $PrBa_2Cu_3O_{7-\delta}$  is identical ( $\sim 165$  ps) and close to the theoretical value. For these reasons a two-dimensional angular correlation of annihilation radiation (2D-ACAR) spectrum was measured in  $YBa_2Cu_3O_7$  at  $T = 400$  K. The spectrum width confirms the delocalization of the positron and the 2D-ACAR shows, apart from the one-dimensional Fermi surface due to CuO chains, a smaller Fermi surface sheet centered around the  $S$  point, in the first Brillouin zone.

### I. INTRODUCTION

Positron annihilation has been extensively used to study the high-temperature superconductor (high- $T_c$ )  $YBa_2Cu_3O_{7-\delta}$ . The temperature dependence of the positron lifetime gives information on the effectiveness of the positrons in investigating the bulk properties of this material, and two-dimensional angular correlation of annihilation radiation<sup>1</sup> (2D-ACAR), is a tool for investigating its Fermi surface (FS). Full-potential linear augmented-plane-wave (FLAPW) band-structure calculations<sup>2</sup> predict four FS sheets: two from the  $CuO_2$  plane states, the one-dimensional FS due to the CuO chain states (identified as the “ridge” henceforward) and the smallest FS sheet centered around the  $S$  point (identified as the “pillbox,” the terminology that is used in Ref. 3) with contributions also from chains. In  $YBa_2Cu_3O_{7-\delta}$ , the positron is mainly localized in the interstitial space in the neighborhood of the CuO chains,<sup>3–6</sup> and only the FS features related to the CuO chain states, i.e., the ridge and the pillbox, are expected to be observed by 2D-ACAR. The ridge FS has been clearly identified by 2D-ACAR measurements in untwinned samples<sup>7–10</sup> and even in twinned samples.<sup>11</sup> An indication of a pillbox signal has also been reported.<sup>12</sup> In earlier measurements we reported 2D-ACAR in samples where Y was completely substituted by the rare-earth elements Dy, Ho, and Pr.<sup>14</sup> In all these cases the ridge signal is not affected by the substitutions, even in the  $PrBa_2Cu_3O_{7-\delta}$  compound, where the macroscopic insulating behavior is ascribed to disorder in CuO chains, which, however, remain metallic at the microscopic level.

In this paper, we study the trapping mechanism in  $Y_{1-x}Pr_xBa_2Cu_3O_{7-\delta}$  using temperature-dependent positron lifetime measurements. These measurements suggest that the trap-free region for positrons in  $YBa_2Cu_3O_{7-\delta}$  is above room temperature. We accordingly present results from a 2D-ACAR measurement in  $YBa_2Cu_3O_{7-\delta}$  at  $T = 400$  K.

### II. POSITRON LIFETIME IN $Y_xPr_{1-x}Ba_2Cu_3O_{7-\delta}$

Positron-lifetime measurements in high- $T_c$  superconductors in general and in  $YBa_2Cu_3O_{7-\delta}$  in particular are

known to be highly dependent on sample preparation methods due to the sensitivity of the positron to defects that are legion in most samples of these materials, whether ceramic or crystalline.<sup>15</sup> It is now accepted that temperature-dependent characteristics of such measurements are due to more or less complicated mechanisms of trapping and detrapping in various traps, especially in “shallow” oxygen vacancies,<sup>16</sup> which could typically give rise to the low-energy detrapping observed. This behavior needs to be understood at least qualitatively to be able to extract information about electronic structure and also so as to better analyze 2D-ACAR spectra. Furthermore, earlier 2D-ACAR measurements on a  $PrBa_2Cu_3O_{7-\delta}$  single crystal revealed the presence of the ridge FS originating in the Cu-O chains, and it would be interesting to verify if lifetime measurements bear out this observation.

A study of the temperature-dependent lifetime in  $Y_{1-x}Pr_xBa_2Cu_3O_{7-\delta}$  samples was undertaken with these aims in mind. The  $Y_{1-x}Pr_xBa_2Cu_3O_{7-\delta}$  system provides several advantages for such a study. It has been extensively investigated from the sample preparation and characterization point of view.<sup>17</sup> As the concentration of Pr is varied, the  $T_c$  drops monotonically to zero for  $x \sim 0.57$ . The sample preparation can be essentially identical for the whole range of  $x$ , as the system remains stable, and this is important if comparative measurements are to be performed. We prepared specimens of  $Y_{1-x}Pr_xBa_2Cu_3O_{7-\delta}$  for  $x = 0.0, 0.2, 0.4, 0.6, 0.8,$  and  $1.0$  (identified henceforward as X00, X02, X04, X06, X08, and X10, respectively) using the solid-state reaction of the appropriate amounts of high purity (99.98% or better)  $Y_2O_3$ ,  $Pr_6O_{11}$ ,  $BaCO_3$ , and  $CuO$ . The precise method used was that given by Neumeier and Maple.<sup>18</sup> It involved five 24-h firing (at 930°C in air) and regrinding stages of the powders followed by three more such stages of increasing duration. Finally the samples were pressed into pellets and annealed in 1 atm of oxygen for two days at 955–970°C, followed by a slow cooling at 1°C/min to 450°C with an 18-h stop and a final slow cool to room temperature. According to Neumeier and Maple, such a treatment produces an oxygen content of  $\sim 6.95$ . The samples were further characterized by x-ray diffraction

and ac susceptibility measurements ( $\chi_{ac}$ ), which gave an indication of their good quality and did not indicate any presence of secondary phases (less than 5%, which is the sensitivity of these methods). The critical temperatures obtained for the superconducting samples were  $T_c = 91$  K (X00),  $T_c = 73$  K (X02), and  $T_c = 41$  K (X04). The other samples were not superconducting. The mass densities obtained for the final samples were approximately 90%.

Temperature-dependent lifetime measurements were performed using a standard lifetime spectrometer (Phillips XP2020Q photomultiplier tubes and plastic scintillators), and a closed-circuit refrigerator. The source used was  $^{22}Na$  deposited on a  $2\mu$ -thick Ni foil with a strength of about  $40 \mu Ci$ . The temperature range investigated was from 40 or 60 K to 300 K with statistics of  $(1.2-1.5) \times 10^6$  for the  $T < 300$  K spectra, and  $2.2 \times 10^6$  for the 300 K spectra. Samples X00 and X10 were also measured at higher temperatures with statistics of  $1.2 \times 10^6$ .

The spectra were analyzed using the MELT program,<sup>19</sup> which uses a Bayesian approach and the maximum entropy principle to solve the inverse problem of extracting the lifetimes and intensities from a multiexponential decay curve. The resolution function was a single Gaussian of full width at half maximum (FWHM)  $\sim 285$  ps. For all samples except X10, in the (40–300)-K temperature range, we find at least two components (apart from the source component) in the spectrum. We deduce this from the intensity distributions for the lifetimes obtained by MELT, which are much wider or clearly indicate two maxima. As an example, see the difference between the distributions at 120 and 430 K for X00 in Fig. 1(b). However, these components are very closely spaced (very often in a range of about 100 ps or less) and attempts to separate them are unstable and the errors on the result very large. We accordingly analyze only the variation of the mean lifetime as a function of temperature, as this quantity is determined quite precisely. A source component (400–410 ps, 5%) was determined using spectra measured at temperatures greater than 400 K, which contained a single well-separated component due to the sample (see below) and subtracted from the spectra at all temperatures. In addition a low intensity, high lifetime component ( $\sim 1200-1500$  ps,  $< 0.3\%$ ) was present in all spectra and is not considered in what follows.

The variation of the mean lifetime as a function of temperature for all six samples is presented in Fig. 2. The following can be seen.

(a) All samples except X10 show a strong variation in the mean lifetime with temperature. The samples with intermediate substitution of Pr ( $0.0 < x < 1.0$ ) have a maximum in the mean lifetime in the range 120–160 K with the lifetime decreasing for both higher and lower temperatures. This behavior could be ascribed to the presence of secondary phases not present in proportions high enough to emerge in the powder-diffraction spectra or, more probably, to complicated trapping and detrapping processes, since these compounds are Y-Pr alloys. Very similar behavior has been observed in alloys of  $YBa_2(Cu_{1-x}M_x)_3O_{7-\delta}$ ,  $M = Ni, Zn$  alloys and has also been ascribed to such processes.<sup>20</sup> However, at a given

temperature, the mean lifetime decreases as the Pr content increases.

(b) Sample X00 has a high mean lifetime ( $\sim 195$  ps) at low temperature and this lifetime decreases monotonically when the temperature is increased, to about 180 ps at room temperature. Sample X10, however, shows no variation of the mean lifetime (165 ps) and a single component is found at all temperatures [Fig. 1(a)]. It is to be noted that theoretical calculations for  $YBa_2Cu_3O_{7-\delta}$  predict a bulk lifetime in the range 157–165 ps.<sup>16,20,21</sup> Adopting the hypothesis that the high lifetime at low temperatures for  $YBa_2Cu_3O_{7-\delta}$  is a manifestation of traps, and the decrease as the temperature increases a manifestation of thermal detrapping, we decided to measure the lifetime at higher temperatures. As expected, we found that the mean lifetime decreases to attain  $\sim 164$  ps at temperatures higher than 360 K and that it remains constant thereafter (till 500 K). What is more, the shape of the intensity curve indicates that we now have a single component [Fig. 1(b)], indicating a progressive delocalization of the positron. The mean lifetime in  $PrBa_2Cu_3O_{7-\delta}$  remains constant for higher temperatures.

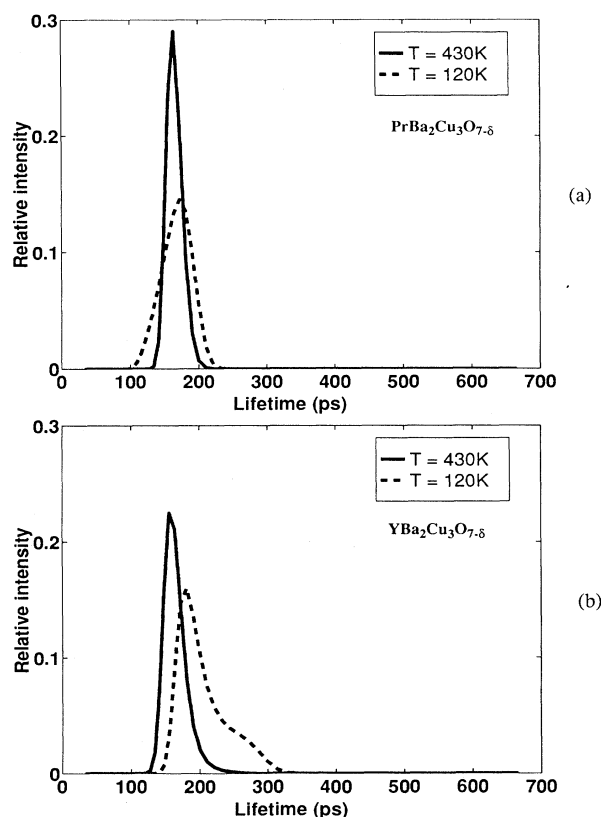


FIG. 1. The intensity curve obtained from the MELT program for the positron lifetime in (a)  $PrBa_2Cu_3O_{7-\delta}$  (sample X10) at  $T = 430$  and 120 K, and (b)  $YBa_2Cu_3O_{7-\delta}$  (sample X00) at  $T = 430$  and 120 K. In  $PrBa_2Cu_3O_{7-\delta}$  there is only one component at both temperatures, with a lifetime of 165 ps. For  $YBa_2Cu_3O_{7-\delta}$  at lower temperatures there is more than one component, while at  $T = 430$  K only one component persists, indicating detrapping and the lifetime decreases to that found in  $PrBa_2Cu_3O_{7-\delta}$ .

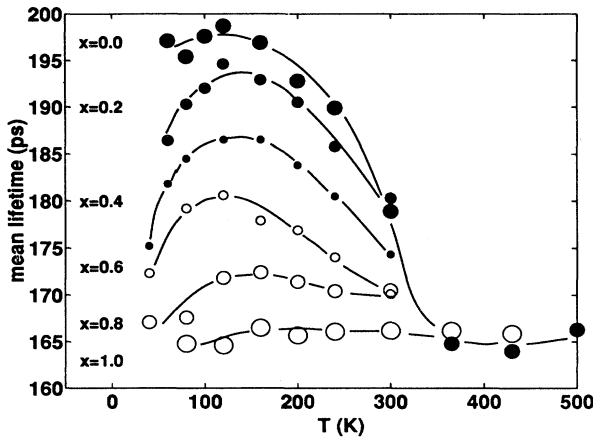


FIG. 2. Mean lifetime as a function of temperature for different concentrations of Pr ( $x=0.0-1.0$ ), in  $Y_{1-x}Pr_xBa_2Cu_3O_{7-\delta}$ . The full circles are for the superconducting samples and the empty ones for the nonsuperconducting ones. The lines are a guide for the eye. The error on each value of the mean lifetime is  $\pm 2$  ps. All samples were measured from 40 or 60 to 300 K and the samples with  $x=0.0$  (X00) and  $x=1.0$  (X10) were further measured at higher temperatures. The absence of variations for X10 with temperature indicates no effects due to positron trapping, while the lowering of the lifetime with temperature for X00 indicates thermal detrapping.

We note also that the mean lifetime at low temperatures and its variation are dependent on the sample preparation and do vary for samples prepared in different ways. These factors suggest that the trapping is essentially due to variations in oxygen content, inhomogeneity or ordering, and not due to twin boundaries or grain boundaries<sup>22</sup> as these are equally present in the  $PrBa_2Cu_3O_{7-\delta}$  compound. Additionally, there is some evidence to suggest that for slow-cooled samples (this being the oxygenation method used for our ceramics as well as single crystals), even well-oxygenated samples may contain oxygen-deficient phases,<sup>23,24</sup> which could trap positrons at low temperatures. Another possibility is that defects might be present in  $PrBa_2Cu_3O_{7-\delta}$  too but may not trap positrons due to a positive charge state.

(c) The mean lifetime for the delocalized positron (which is in fact the bulk lifetime) in  $YBa_2Cu_3O_{7-\delta}$  and  $PrBa_2Cu_3O_{7-\delta}$  is identical. It is known from calculations<sup>5</sup> and experiments<sup>14</sup> that the positron samples essentially the electronic structure in the chains and preliminary calculations show that this is true also for  $PrBa_2Cu_3O_{7-\delta}$ . We conclude that the chains in both compounds are similar in behavior, confirming the earlier 2D-ACAR result for single crystals. This is also in agreement with optical reflectivity measurements<sup>25</sup> and with recent measurements of resistive transition in  $YBa_2Cu_3O_{7-\delta}/PrBa_2Cu_3O_{7-\delta}$  superlattices.<sup>26</sup> It is to be noted that these results are compatible with the theoretical model of Fehrenbacher and Rice<sup>27</sup> in which the chains in  $PrBa_2Cu_3O_{7-\delta}$  are microscopically similar to those in  $YBa_2Cu_3O_{7-\delta}$ .

(d) It would be worthwhile to measure the 2D-ACAR spectrum in  $YBa_2Cu_3O_{7-\delta}$  at temperatures around 400 K to see if this trend is reproduced in single crystals and also with the hope that delocalization may give rise to sharper FS features. A temperature-dependent 2D-ACAR study was performed earlier by Smedskjaer *et al.*<sup>12</sup> showing a variation in the 2D-ACAR spectra from 30 to 300 K; however we have seen that at 300 K positrons are still not delocalized completely. The lifetime measurements are on ceramic material but it is not likely that the trends discovered are valid also for single crystals, especially since the high density of our samples suggests similarities with single crystals as far as oxygenation problems are concerned.

### III. 2D-ACAR IN $YBa_2Cu_3O_{7-\delta}$ AT 400 K

Our 2D-ACAR setup was described earlier in detail.<sup>13</sup> The measurements presented here were made under vacuum ( $< 10^{-5}$  Torr), using a 40-mCi  $^{22}Na$  positron source and a magnetic field of 4 T to focus the positrons onto the sample. The data acquisition rate varied between 330 and 400 events/s depending on the sample measured, the sample-detector distance being 4.98 m. The FWHM of angular resolution of the apparatus taking only geometrical considerations into account is about  $0.65 \times 0.65$  mrad.<sup>2</sup> This further increases to about  $0.85 \times 0.85$  mrad<sup>2</sup> for the maximum measurement temperature of 400 K.

A 2D-ACAR measurement at a temperature of 400 K was performed on a good quality untwinned  $YBa_2Cu_3O_{7-\delta}$  crystal (YBCO400K), which was measured earlier under different conditions.<sup>14</sup> The total number of counts in the spectrum was  $2.3 \times 10^8$ . This was sufficient to detect the third umklapp signature of the ridge FS,<sup>14</sup> attesting to the statistical quality of the data. In Figs. 3(a) and 3(b) we compare normalized sections of the 2D-ACAR along the  $p_a$  ( $p_a$  is the momentum in the  $2\pi/a$  direction) and  $p_b$  directions for this measurement, an earlier measurement at 300 K (YBCO300K) and the theoretical FLAPW calculations convoluted with the experimental resolution function. It can be seen that at 400 K the measured spectrum is wider, indicating a more delocalized positron and a shorter lifetime. However, comparison with the theoretical curves shows that the amplitude of the FS features is still more significant in the calculations as compared to experiments. In Fig. 3(c) we compare the widths of the artificially twinned  $YBa_2Cu_3O_{7-\delta}$  measurement at 400 K with that of a measurement in  $PrBa_2Cu_3O_{7-\delta}$  at 300 K (PRBCO300K) as lifetime measurements for  $PrBa_2Cu_3O_{7-\delta}$  do not indicate a change in lifetime with temperature. The curves are practically superposed, again bearing out our lifetime result. A quantitative way to compare these widths precisely is the evaluation of the shape factor  $S$  (the untwinned measurements were artificially folded to simulate twinning for this comparison). We define it as the 2D-ACAR volume contained in a central window ( $\pm 3.6$  mrad) of a 2-mrad-wide slice along  $p_a$  or  $p_b$ , divided by the total volume ( $\pm 26$  mrad) of the slice. A large  $S$  factor results from a narrow 2D-ACAR spectrum. The  $S$  factors for PRBCO20K, PRBCO300K, YBCO400K, and YBCO300K are, respec-

tively, 0.5119, 0.5137, 0.5143, and 0.5238, with a statistical error smaller than  $2 \times 10^{-4}$ . The  $T_c$  of the sample was measured before and after the 400-K measurement and showed no deterioration, indicating no deoxygenation, which occurs at temperatures significantly higher than 400 K.<sup>28</sup>

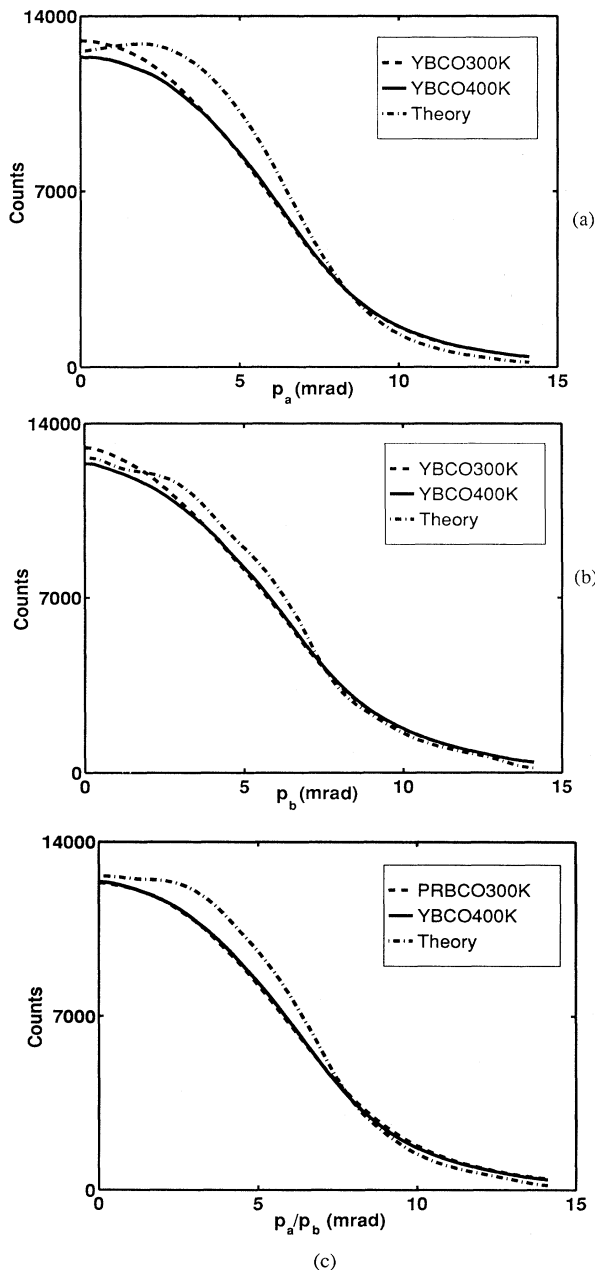


FIG. 3. Sections through normalized (to  $1 \times 10^8$  counts) 2D-ACAR spectra. All spectra have been smoothed by a  $0.75 \text{ mrad} \times 0.75 \text{ mrad}$  constant square function. (a) and (b) are sections along  $p_a$  and  $p_b$ , respectively. The YBCO400K measurement is wider than YBCO300K indicating delocalized positrons. (c) Sections through twinned spectra (twinning simulated for theory and YBCO400K) showing that YBCO400K and PRBCO300K are practically superposed as expected from the lifetime results.

With the assurance that the positron is indeed delocalized at 400 K, we looked for FS features in this measurement. The ridge FS being already well characterized, we looked for traces of the pillbox FS, around the  $S$  point. There was an earlier report<sup>12</sup> of the detection of the pillbox signature in the second Brillouin zone (BZ). In Fig. 4 sections along the BZ edge ( $p_a = 3.15 \text{ mrad}$ ) of the anisotropic part of the 2D-ACAR spectra are presented for YBCO300K, YBCO400K, and the FLAPW calculations divided by a factor of 3. This second BZ pillbox signature is clearly visible in the calculations but completely absent in YBCO300K. In YBCO400K, a small dip appears at the expected point, but it is not significant when compared to the error bars. However, this measurement does present sharper features than YBCO300K. We conclude that the pillbox signature must be sought for in the first BZ, where the statistics are higher. However, care must be taken to distinguish it from modulations result-

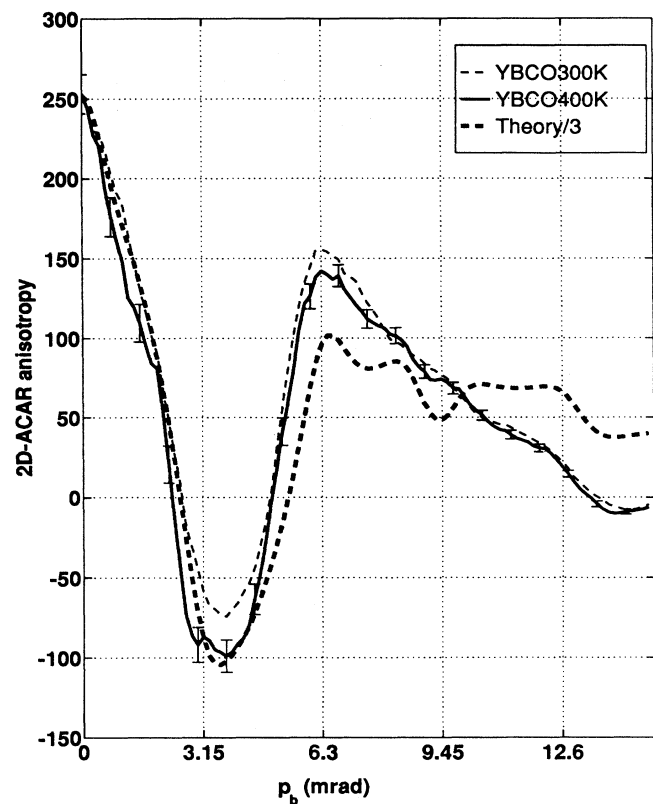


FIG. 4. Sections through the anisotropic part of the 2D-ACAR spectra for YBCO300K, YBCO400K, and FLAPW calculations for  $p_a = 3.15 \text{ mrad}$ , along the edge of the first Brillouin zone (BZ). All spectra were smoothed by a  $0.75 \text{ mrad} \times 0.75 \text{ mrad}$  constant square function, and the theoretical curve was further convolved with the experimental resolution, divided by a factor of 3, and shifted for convenient presentation. The x-axis ticks are spaced by half the BZ width. For  $9 \text{ mrad} < p_b < 10 \text{ mrad}$ , theory predicts a dip corresponding to the pillbox FS, absent in YBCO300K, and not statistically significant in YBCO400K. The error bars (shown only for YBCO300K—they are smaller for YBCO400K) also represent statistically uncorrelated points.

ing from the overlap of the positron with the filled bands (wave-function effects), which are known to be strong in the first BZ.

We accordingly applied to the first BZ a filtering technique,<sup>29</sup> which extracts breaks in the 2D-ACAR distribution. The results for FLAPW calculations, YBCO400K, and YBCO300K are presented in Fig. 5, where the vertical axis indicates the amplitude of the structure and the horizontal axes indicate its position and width. The large intensity along the  $p_a$  axis with a narrow width for the break is due to the ridge FS. It is clearly seen that the amplitudes of the structures in experiment are smaller by

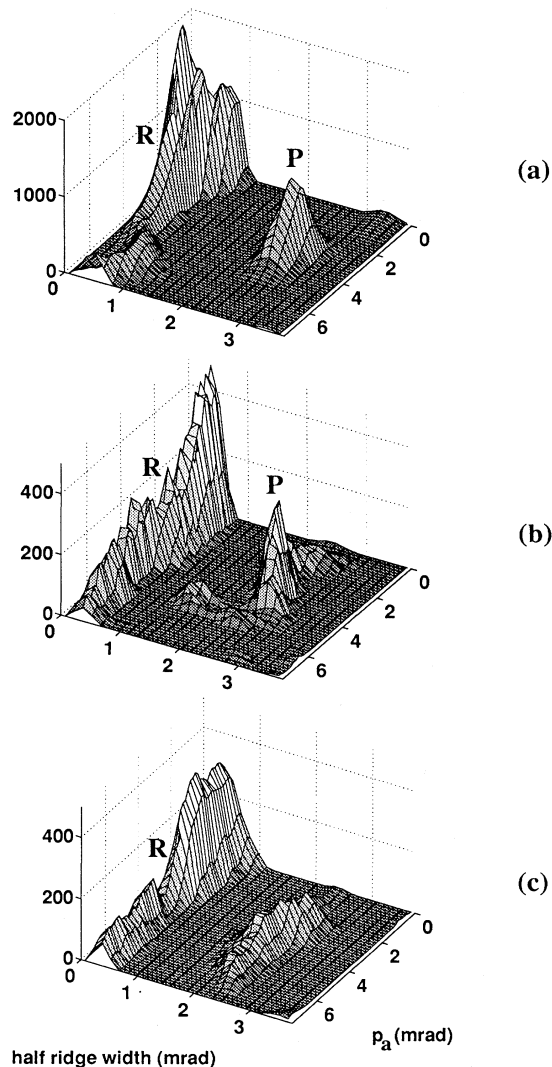


FIG. 5. Output of a filter for extracting breaks in the 2D-ACAR spectra. The vertical axis represents intensities of such structures, and the horizontal plane situates the structures in the momentum space (see text for more details). The filter was applied to the first BZ. (a) FLAPW theory. The intense peak corresponding to a narrow ridge width indicates the ridge FS (labeled *R*), while the smaller peak corresponds to the pillbox FS (labeled *P*). (b) Both of these FS signatures are present in YBCO400K. (c) In YBCO300K the pillbox peak disappears, probably masked by positron trapping.

a factor of 5 than those predicted by theory. The ridge signal, though clearly visible for both YBCO300K and YBCO400K, is stronger by a factor 1.5 in the latter. The theory predicts a smaller intensity break at  $p_a \sim 3$  mrad corresponding to the pillbox FS. In YBCO300K there is a smooth modulation probably containing a pillbox signal masked by positron trapping. In YBCO400K a sharp peak corresponding to the pillbox FS emerges clearly and compares well with the theoretical prediction.

As seen before, the YBCO400K, PRBCO300K, and PRBCO20K spectra are almost identical in width. Another way of getting rid of the unwanted background and modulations in the YBCO400K measurement (including the now familiar ridge FS) is to simply subtract from it the PRBCO300K or the PRBCO20K spectrum (again all operations are performed on normalized spectra). As the  $\text{PrBa}_2\text{Cu}_3\text{O}_{7-\delta}$  measurements are twinned, YBCO400K was artificially folded (to simulate twinning) before this operation. A quarter of the first BZ after subtraction is shown in Fig. 6. It can be seen that a sharp

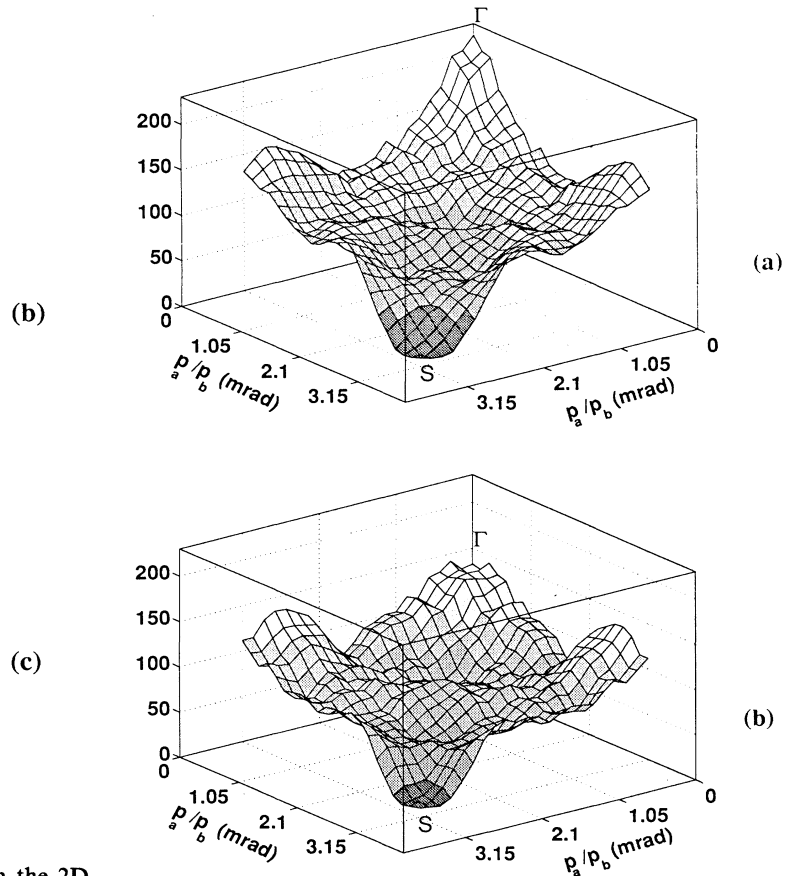


FIG. 6. 2D-ACAR differences obtained by subtracting (a) PRBCO20K and (b) PRBCO300K, from YBCO400K. The figures show a quarter of the first BZ. Structure appears, corresponding to FS features extending in  $\text{YBa}_2\text{Cu}_3\text{O}_{7-\delta}$  but not in  $\text{PrBa}_2\text{Cu}_3\text{O}_{7-\delta}$ . A break is seen at the *S* point in the corner of the BZ, where the pillbox signature is expected. PRBCO20K and PRBCO300K are twinned, while YBCO400K was folded to simulate twinning. The error on the vertical scale is  $\pm 12$  counts.

dip is obtained at the corner corresponding to the  $S$  point. This break is significantly larger than the error ( $4\sigma$ ) even though it is very small compared to the maximum of the 2D-ACAR (about 0.5%). Apart from confirming the presence of the pillbox FS in  $YBa_2Cu_3O_{7-\delta}$  this would indicate that this FS is not present in  $PrBa_2Cu_3O_{7-\delta}$ . FLAPW band-structure calculations have recently been performed for this compound with the following conclusions.<sup>30</sup> The band structure is qualitatively similar, with several differences. The ridge FS is wider as compared to  $YBa_2Cu_3O_{7-\delta}$  and the pillbox FS disappears for the non-spin-polarized calculation. It, however, reappears for the spin-polarized calculation. Other features, significant when compared to the error, do appear in the difference spectrum, but it must be remembered that the measurements are twinned and these features might be due to the twinning procedure so we do not interpret them for the moment. High statistics measurements on untwinned crystals, which will help to deal with these questions, are now in progress and will be reported on shortly.

Though there has been considerable progress in the understanding of positron annihilation data in  $YBa_2Cu_3O_{7-\delta}$  in the past few years, some important questions remain. It is intriguing that the Fermi surface structures present in the data agree by and large, with those predicted by theory but are systematically weaker, by a factor of about 5 in the first BZ (see Fig. 5) even when the positrons are delocalized, and that the anisotropy is smaller by a factor of about 3 in the experiment as compared to the theory (Fig. 4). Moreover, comparison of sections (Fig. 3) through theoretical and experimental spectra still show differences, for example in Fig. 3(b) the theoretical spectrum has a hump around 2.5 mrad, which

is absent in experiment. Including effects of annihilation in the core regions changes the 2D-ACAR spectrum very little and hence does not improve the match between theory and experiment. These inconsistencies could be due to electron-electron correlation effects not included in the calculation. These effects are expected to reduce the amplitude of FS breaks,<sup>6</sup> a phenomenon observed in Compton profile measurements of copper.<sup>31</sup>

#### IV. CONCLUSIONS

In conclusion, we have shown that positron trapping, probably due to oxygen vacancies, is negligible in  $PrBa_2Cu_3O_{7-\delta}$ , and that though positrons are trapped in such vacancies at lower temperatures in  $YBa_2Cu_3O_{7-\delta}$ , they are essentially delocalized for temperatures greater than 360 K. Furthermore, the lifetimes for delocalized positrons are identical for  $PrBa_2Cu_3O_{7-\delta}$  and  $YBa_2Cu_3O_{7-\delta}$  and consistent with theoretical predictions, indicating a similar electronic character in the chains and bearing our earlier 2D-ACAR results.<sup>14</sup> In a 2D-ACAR spectrum measured at 400 K in  $YBa_2Cu_3O_{7-\delta}$ , we observe the signature in the first BZ of the small FS sheet centered around the  $S$  point and conclude also that this FS feature is probably absent in  $PrBa_2Cu_3O_{7-\delta}$ .

#### ACKNOWLEDGMENTS

We thank W. N. Hardy for having supplied us with a high quality  $YBa_2Cu_3O_{7-\delta}$  sample and Dr. S. Massidda for interesting discussions. This work was supported by the Swiss National Science Foundation.

\*Present address: Laboratory of Physics, Helsinki University of Technology, 02150 Espoo, Finland.

<sup>1</sup>S. Berko, in *Momentum Distributions*, edited by R. N. Silver and P. E. Sokol (Plenum, New York, 1989); M. Peter, *IBM J. Res. Develop.* **33**, 333 (1989).

<sup>2</sup>S. Massidda, J. Yu, A. J. Freeman, and D. D. Koelling, *Phys. Rev. Lett. A* **122**, 198 (1987).

<sup>3</sup>A. Bansil, P. E. Mijnaerends, and L. C. Smedskjaer, *Phys. Rev. B* **43**, 3667 (1991).

<sup>4</sup>D. Singh, W. E. Pickett, E. C. von Stetten, and S. Berko, *Phys. Rev. B* **42**, 2696 (1990).

<sup>5</sup>S. Massidda, *Physica C* **169**, 137 (1990).

<sup>6</sup>T. Jarlborg, B. Barbiellini, E. Boronski, P. Genoud, and M. Peter, *J. Phys. Chem. Solids* **52**, 1515 (1991).

<sup>7</sup>L. C. Smedskjaer, A. Bansil, U. Welp, Y. Fang, and K. G. Bayl, *J. Phys. Chem. Solids* **52**, 1541 (1991).

<sup>8</sup>H. Haghghi, J. H. Kaiser, S. Rayner, R. N. West, J. Z. Liu, R. Shelton, R. H. Howell, F. Solar, P. A. Sterne, and M. J. Fluss, *J. Phys. Chem. Solids* **52**, 1535 (1991); *Phys. Rev. Lett.* **67**, 38 (1991).

<sup>9</sup>A. A. Manuel, B. Barbiellini, M. Gauthier, L. Hoffmann, T. Jarlborg, S. Massidda, M. Peter, W. Sadowski, A. Shukla, and E. Walker, *J. Phys. Chem. Solids* **54**, 1223 (1993).

<sup>10</sup>L. Hoffmann, A. A. Manuel, B. Barbiellini, M. Peter, A.

Shukla, and E. Walker, *Acta Phys. Polonica A* (to be published).

<sup>11</sup>M. Peter, A. A. Manuel, L. Hoffmann, and W. Sadowski, *Europhys. Lett.* **18**, 313 (1992).

<sup>12</sup>L. C. Smedskjaer, A. Bansil, U. Welp, Y. Fang, and K. G. Bayle, *Physica C* **192**, 259 (1992).

<sup>13</sup>P. E. Bisson, P. Descouts, A. Dupanloup, A. A. Manuel, E. Perreard, M. Peter, and R. Sachot, *Helv. Phys. Acta* **55**, 100 (1982).

<sup>14</sup>L. Hoffmann, A. A. Manuel, M. Peter, E. Walker, M. Gauthier, A. Shukla, B. Barbiellini, S. Massidda, Gh. Adam, S. Adam, W. N. Hardy, and Ruixing Liang, *Phys. Rev. Lett.* **71**, 4047 (1993).

<sup>15</sup>R. M. Nieminen, *J. Phys. Chem. Solids* **52**, 1577 (1991).

<sup>16</sup>K. J. Jensen, R. M. Nieminen, and M. J. Puska, *J. Phys. Condens. Matter* **1**, 3727 (1989).

<sup>17</sup>A. Kebede, C. S. Jee, J. Schwegler, J. E. Crow, T. Mihalisin, G. H. Myer, R. E. Salomon, P. Schlottmann, M. V. Kuric, S. H. Bloom, and R. P. Guertin, *Phys. Rev. B* **40**, 4453 (1989), and references therein.

<sup>18</sup>J. Neumeier and M. B. Maple, *Physica C* **191**, 158 (1992).

<sup>19</sup>A. Shukla, M. Peter, and L. Hoffmann, *Nucl. Instrum. Methods A* **335**, 310 (1993).

<sup>20</sup>S. Ishibashi, R. Yamamoto, M. Doyama, and T. Matsumoto,

- J. Phys. Condens. Matter **3**, 9169 (1991).
- <sup>21</sup>T. McMullen, P. Jena, S. N. Khanna, Y. Li, and K. J. Jensen, Phys. Rev. B **43**, 10422 (1991).
- <sup>22</sup>D. Hentrich, J.-E. Kluin, and Th. Hehenkamp, Phys. Status Solidi B **172**, 99 (1992).
- <sup>23</sup>L. E. Levine and M. Daumling, Phys. Rev. B **45**, 8146 (1992).
- <sup>24</sup>J. Mesot, P. Allenspach, U. Staub, and A. Furrer (unpublished).
- <sup>25</sup>K. Tanaka, Y. Imanaka, K. Tamasaku, T. Ito, and S. Uchida, Phys. Rev. B **46**, 5833 (1992).
- <sup>26</sup>Y. Suzuki, J.-M. Triscone, C. B. Eom, M. R. Beasley, and T. H. Geballe, Phys. Rev. Lett. **73**, 328 (1994).
- <sup>27</sup>R. Fehrenbacher and T. M. Rice, Phys. Rev. Lett. **70**, 3471 (1993).
- <sup>28</sup>See, for example, K. Conder, Ch. Kruger, E. Kaldis, D. Zech, and H. Keller, Physica C **225**, 13 (1994).
- <sup>29</sup>L. Hoffmann, A. Shukla, M. Peter, B. Barbiellini, and A. A. Manuel, Nucl. Instrum. Methods A **335**, 276 (1993).
- <sup>30</sup>D. J. Singh, Phys. Rev. B **50**, 4106 (1994).
- <sup>31</sup>J. R. Schneider and F. Bell, Europhys. News **23**, 10 (1992).